Magnetoexchange Branches and Spin-Wave Resonance in Conducting and Insulating Films: Perpendicular Resonance

T. Wolfram and R. E. De Wames
North American Rockwell Science Center, Thousand Oaks, California 91360
(Received 26 April 1971)

Spin-wave modes in thin ferromagnetic metallic plates or films are characterized by a wave vector $k_{\parallel}$ parallel to the sample surface in addition to the standing spin-wave mode number n which designates the number of half-wavelengths across the sample. The dependence of the spin-wave frequency on $k_{\parallel}$ is principally due to dipolar effects similar to those encountered in magnetostatic theory. Analytic expressions for the frequencies $\Omega_n(k_{\parallel})$ of the spin-wave modes including the effects of exchange, dipolar interactions, eddy currents, and phenomenological relaxation are derived for the case in which the applied magnetic field is perpendicular to the film surface and the spins are pinned. The dispersion branches $\Omega_n(k_{\parallel})$ (for fixed n) are referred to as magnetoexchange branches since they are both magnetostatic and exchangelike in nature. The magnetoexchange dispersion for an insulating sample is also obtained and shown to be quite different from that of the metallic case. A general theory for the surface impedance $Z(\omega, k_{\parallel})$ is developed which reduces to the usual surface impedance when $k_{\parallel} \to 0$. Simple analytical expressions for the spin-wave resonance power absorption peaks of thin metallic films are obtained. The intensity I_n of the spin-wave peak absorption is shown to be independent of n in the absence of phenomenological relaxation. For nonvanishing relaxation, $I_n \propto 1/n^2$. The "peak-to-valley" difference of the derivative $\partial I_n/\partial H_{app}$ behaves in the same way. Small variations in film thickness lead to the result that $\partial I_n/\partial H_{app} \propto 1/n^4$ instead of $1/n^2$. Simple analytical expressions are also obtained for the surface impedance of thick films. The ferromagnetic resonance (FMR) peak is shifted upward from the magnetostatic result $\Omega = \Omega_H$. Expressions are given for the dipolar dispersion of the FMR peak as a function of $k_{\parallel}$. The curve is linear for small $k_{\parallel}$ with a slope much smaller than that of an equivalent magnetostatic branch in an insulator. The power absorption associated with the right-hand circularly polarized h_{rf} component has a deep minimum at $\omega = \gamma H_{app}$ which is associated with the phenomena of transmission resonance in metallic films.

I. INTRODUCTION

Ferromagnetic resonance experiments on metallic ferromagnets have received considerable attention since the initial experiments by Griffiths[1] and Yager and Bozorth.[2] Such experiments gave valuable information concerning the g factor and magnetic relaxation.[3] Rado and Weertman[4] and Ament and Rado[5] demonstrated experimentally and theoretically that the exchange interaction leads to a measurable shift in the ferromagnetic resonance (FMR) peak. This "exchange shift" was used to calculate the exchange stiffness or exchange constant for the metallic ferromagnet. Ament and Rado[5] suggested that the name "spin-wave resonance" was appropriate since the exchange interaction plays a vital role.

Standing spin waves in thin ferromagnetic films were first observed by Seavey and Tannenwald[6] and subsequently by numerous other workers.[7] These spin-wave modes are characterized by the number of half-wavelengths n across the film with the wave vector $k_{\parallel}$ parallel to the film surface zero. Theoretical analyses of these spin-wave resonances have been given by many authors.[8-10]

The purpose of this work is to investigate the dependence of the spin-wave frequencies on $k_{\parallel}$ for metallic and insulating films. General expressions for the power absorption for $k_{\parallel} \neq 0$ are developed and analyzed. The $k_{\parallel} = 0$ surface impedance is analyzed in great detail and a number of (hopefully) useful approximate expressions are derived.

It is well appreciated that the microwave absorption spectrum is dependent upon the details of the boundary conditions[10,11] satisfied by the magnetization. We have chosen here to treat in detail the particular situation in which the rf magnetization vanishes at the surface of the sample (i.e., the spins are pinned). For metallic ferromagnetic films a high degree of spin pinning appears to be a frequently occurring experimental situation.[7,8]

We refer to the dependence of the spin-wave modes on $k_{\parallel}$ as *dipolar dispersion*, since for small values of $k_{\parallel}$ the dipolar energy dominates the exchange energy. The importance of dipolar dispersion has been illustrated for insulating films such as yttrium iron garnet (YIG). Recent experiments[12] on epitaxial YIG films have been reported in which a series of resonances associated with quantized values of $k_{\parallel}$ was observed. The dipolar dispersion of YIG deduced from these resonances is in qualitative agreement with theory.[13] The quantized wavelengths associated with the modes are

approximately multiples of the sample width W and length L. The spectrum agrees well with $k_{\parallel} = (m\pi/W, p\pi/L)$ where m and p are integers. In contrast to the usual spin-wave resonances in thin metallic films the YIG resonances correspond approximately to a uniform spin excitation amplitude across the film. In this case n is not a good quantum number for the magnetostatic modes.[13]

Evidence for dipolar dispersion and geometrical quantization of $k_{\parallel}$ in metallic ferromagnets has been reported recently by Phillips *et al.*[14] They observed spin-wave resonances in small single-crystal dendritic platelets of Ni and Ni-Fe alloys whose dispersion appears to be principally magnetostatic in origin.

In Sec. II, a set of equations for a conducting ferromagnetic plate is obtained from Maxwell's equations and the equations of motion for the magnetization. This set of equations includes the dipole-dipole interactions, exchange interaction, conduction processes (eddy currents), and phenomenological relaxation of the magnetization. The general equations are then expressed as a symmetrized matrix equation and the fundamental vector solutions are given. In Sec. III, the spin-wave eigenvalue problem is discussed. Solutions for the case in which the applied magnetic field is perpendicular to the sample surface and the spins are pinned are derived. The spin-wave modes are characterized by n the number of half-wavelengths across the film thickness and by $k_{\parallel}$ the "in-plane" propagation vector. The dispersion curve $\Omega_n(k_{\parallel})$ for the spin-wave frequencies as a function of $k_{\parallel}$ for fixed n is referred to as a magnetoexchange branch. For small $k_{\parallel}$ the dispersion of $\Omega_n(k_{\parallel})$ is principally due to dipolar effects (dipolar dispersion). Analytical expressions for the magnetoexchange branches of both metallic and insulating films are derived. For metallic samples all magnetoexchange branches possess an initial linear dependence on $k_{\parallel}$. In insulating films only the odd modes (n = odd integer) have a linear slope. The even modes have a quadratic dispersion for small $k_{\parallel}$. For pinned boundary conditions the usual *magnetostatic* branch of the insulator does not occur.

Section IV addresses the problem of the microwave absorption in a uniform rf linearly polarized magnetic field. General expressions for the power absorption are derived from Poynting's theorem. A generalized surface impedance $Z(\omega, k_{\parallel})$ is defined to treat the case in which $k_{\parallel} \neq 0$. The properties of the $k_{\parallel} = 0$ surface impedance are derived. In Sec. V the characteristics of the power absorption spectrum are discussed. The absorption is resolved into a FMR background including eddy currents plus a spin-wave resonance contribution. Simple analytic expressions are derived for each contribution for thin samples. The intensity of the spin-wave resonance I_n and the derivative of the intensity $\partial I_n/\partial H_{\text{app}}$ are discussed.

It is found that the I_n is constant for varying n when magnetic relaxation is absent but varies as $1/n^2$ when relaxation is present. The derivative $\partial I_n/\partial H_{\text{app}}$ behaves in the same fashion. The "peak-to-valley" difference in $\partial I_n/\partial H_{\text{app}}$ varies as $1/n^2$ for a uniformly thick film. Variations in film thickness as small as 1% lead to a $1/n^4$ dependence.

The characteristics of the FMR peak are studied for thick specimens. Simple expressions are derived for describing the FMR peak and its dependence on $k_{\parallel}$. The FMR peak shifts linearly with $k_{\parallel}$ for small $k_{\parallel}$. At high frequencies an absorption minimum occurs at $\omega = \gamma H_{\text{app}}$. This antiresonance is related to the phenomena of magnetic transmission resonance.[15]

II. GENERAL THEORY

A. Maxwell's Equations

In this section we develop the equations for the spin-wave modes of a metal ferromagnetic plate or film.

The metal ferromagnetic sample is infinite in the x and y directions and extends from $-d/2$ to $+d/2$ along the z axis as shown in Fig. 1. A static applied magnetic field $H_{\text{app}} > 4\pi M_s$ directed along the z axis leads to a static internal field $H_0 = H_{\text{app}} - 4\pi M_s$, where M_s is the saturation magnetization. The total field H is $H_0 + h$ where h is a small time-varying component (in the x-y plane) transverse to H_0. In cgs units, Maxwell's equations are

$$\vec{\nabla} \times \vec{h} = \frac{4\pi\sigma}{c}\,\vec{e} \tag{2.1}$$

and

$$\vec{\nabla} \times \vec{e} = -\frac{1}{c}\,\frac{\partial}{\partial t}\,(\vec{h} + \vec{m})\,, \tag{2.2}$$

where $\vec{e}$ is the electric field and the transverse magnetization $\vec{m}$ includes the usual factor of 4π ($\vec{m} = 4\pi\vec{m}_t$). The quantities σ and c are the electrical conductivity and the velocity of light, respectively. Using Eqs. (2.1) and (2.2) one obtains

$$-\nabla^2\vec{h} + \vec{\nabla}(\vec{\nabla}\cdot\vec{h}) + (2i/\delta^2)(\vec{h} + \vec{m}) = 0\,, \tag{2.3}$$

if the fields vary as $e^{i\omega t}$ in time. The parameter $\delta = (c^2/2\pi\sigma\omega)^{1/2}$ is the classical electromagnetic skin depth.

For the geometry considered here the fields are of the form $e^{i(k_x x + k_y y)} f(k_{\parallel}, z) = e^{i(\vec{k}_{\parallel}\cdot\rho)} f(k_{\parallel}, z)$, where the propagation vector $\vec{k}_{\parallel}$ and the position vector ρ lie in the x-y plane and f varies spatially with z but depends only parametrically on $|k_{\parallel}|$. From Eq. (2.3) we obtain the equations

$$\left(K^2 + 2i - \delta^2\,\frac{\partial^2}{\partial z^2}\right)\begin{pmatrix} h_x \\ h_y \end{pmatrix}$$

$$+\left[\begin{pmatrix} 0 & 1 \\ 1 & 0 \end{pmatrix} K_x K_y + \begin{pmatrix} K_x^2 \\ K_y^2 \end{pmatrix} + 2i\right] \begin{pmatrix} m_x \\ m_y \end{pmatrix} = 0 , \quad (2.4)$$

where

$$K_x = \delta k_x, \quad K_y = \delta k_y , \quad K^2 = \delta^2(k_x^2 + k_y^2) . \quad (2.5)$$

The quantity $D/4\pi$, the exchange constant, is discussed below. The fields $\vec{h}$ and $\vec{m}$ in Eq. (2.4) are functions of $k_\parallel$ and z. The h_z component has been eliminated in obtaining Eq. (2.4) by using the relation

$$h_z = \frac{-i\delta}{(K^2 + 2i)} \frac{\partial}{\partial z} (K_x h_x + K_y h_y) , \quad (2.6)$$

derived from Eq. (2.3).

B. Magnetization Equations

The equations of motion for the magnetization including the phenomenological Landau-Lifshitz relaxation terms[16] are

$$\frac{i\hbar\omega}{4\pi\gamma M_s} \vec{m} = (\vec{1}_z \times \vec{\mathcal{H}}_{eff}) + \frac{1}{\gamma M_s t_1} \vec{\mathcal{H}}_{eff} - \frac{1}{\gamma M_s t_2} [\vec{1}_z \times (\vec{1}_z \times \vec{\mathcal{H}}_{eff})] , \quad (2.7)$$

where γ is the gyromagnetic ratio, $\vec{1}_z$ is a unit vector in the z direction, and τ_1 and τ_2 are phenomenological relaxation times. The effective field[16] is given by

$$\vec{\mathcal{H}}_{eff} = \vec{h} - \left(\frac{H_0}{4\pi M_s} + (\epsilon\delta k_\parallel)^2\right) \vec{m} + (\epsilon\delta)^2 \frac{\partial^2}{\partial z^2} \vec{m} . \quad (2.8)$$

The product $(\epsilon\delta)^2 = D/4\pi$ is the exchange constant for the magnetic medium. It is related to the Landau exchange stiffness A by the relation $D/4\pi = 2A/4\pi M_s^2$. Equations (2.7) and (2.8) yield the relations

$$\frac{\partial^2}{\partial r^2} (m_y - l m_x) + (i\Omega + l\Omega_K) m_x - \Omega_K m_y + h_y - l h_x = 0 ,$$
$$\frac{\partial^2}{\partial r^2} (m_x + l m_y) - (i\Omega + l\Omega_K) m_y - \Omega_K m_x + l h_y + h_x = 0 , \quad (2.9)$$

where

$$\Omega = \frac{\hbar\omega}{4\pi\gamma M_s} ,$$
$$\Omega_K = \frac{H_0}{4\pi M_s} + (\epsilon\delta k_\parallel)^2 ,$$
$$l = \frac{1}{\gamma M_s}\left(\frac{1}{\tau_1} + \frac{1}{\tau_2}\right) \equiv \frac{1}{\gamma M_s \tau} , \quad (2.10)$$
$$r = (\epsilon\delta)^{-1} z .$$

C. Symmetry Reduced Equations

The four equations, Eqs. (2.4) and (2.9), determine the $\vec{h}$ and $\vec{m}$ fields. These equations may be combined into the matrix equation

$$\left(\hat{1} \frac{\partial^2}{\partial r^2} - \hat{B}^2\right) \vec{f} = 0 , \quad (2.11)$$

where $\vec{f}$ is a four vector whose components are $f_1 = h_x$, $f_2 = h_y$, $f_3 = m_x$, $f_4 = m_y$, and $\hat{1}$ is a 4×4 unit matrix. The matrix $\hat{B}^2$ is

$$\begin{bmatrix} g^2 & 0 & \epsilon^2(K_x^2 + 2i) & \epsilon^2 K_x K_y \\ 0 & g^2 & \epsilon^2 K_x K_y & \epsilon^2(K_y^2 + 2i) \\ -1 & 0 & \Omega_k' & i\Omega' \\ 0 & -1 & -i\Omega' & \Omega_k' \end{bmatrix} , \quad (2.12)$$

where $\Omega' = \Omega/(1 + l^2)$, $\Omega_k' = \Omega_k + i\Omega'$, and $g^2 = \epsilon^2(2i + K^2)$. In obtaining Eq. (2.11) we have factored out the matrix

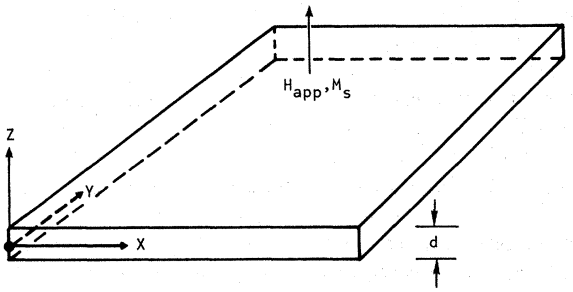

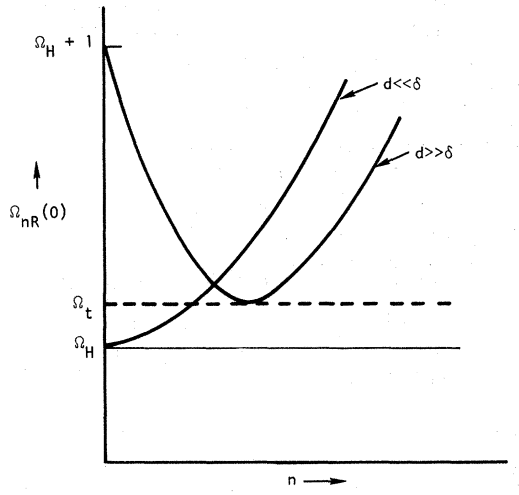

FIG. 1. The coordinate system (upper) for the ferromagnetic plate. The external applied magnetic field H_{app} and the saturation magnetization are oriented along the Z axis. A schematic (lower) of the dependence of the spin-wave frequencies on the number n of half-wavelengths across the thickness of the plate. Dipolar effects lead to a thickness dependence. When d is large compared with the skin depth δ the dispersion curve has a minimum frequency Ω_t.

$$A=\begin{bmatrix}1&0&0&0\\0&1&0&0\\0&0&1&l\\0&0&-l&1\end{bmatrix} \tag{2.13}$$

in order to diagonalize the second-derivative operator.

From the planar symmetry it follows that the fields depend only upon the magnitude of K and not on its individual components. This feature is not obvious from the $\hat{B}^2$ matrix. If we rotate our coordinate system in the x-y plane the symmetry can be made explicit. We accomplish the rotation by a unitary transformation U defined by

$$U=\frac{1}{K}\begin{bmatrix}K_x&K_y&0&0\\-K_y&K_x&0&0\\0&0&K_x&K_y\\0&0&-K_y&K_x\end{bmatrix}, \tag{2.14}$$

where $K=(K_x^2+K_y^2)^{1/2}$. We then obtain the matrix equation

$$\left(\hat{1}\frac{\partial^2}{\partial r^2}-\hat{C}^2\right)\vec{f}'=0, \tag{2.15}$$

where the components of $f'=U^+f$ are h_x', h_y', m_x', and m_y' and

$$\hat{C}^2=U^+B^2U=\begin{bmatrix}g^2&0&g^2&0\\0&g^2&0&\alpha\\-1&0&\Omega_k'&i\Omega'\\0&-1&-i\Omega'&\Omega_k'\end{bmatrix}. \tag{2.16}$$

The quantity $\alpha=2i\epsilon^2$ and $g^2=\alpha+\epsilon^2K^2$. Equation (2.15) explicitly displays the proper symmetry. The rotated fields are

$$\begin{pmatrix}h_x'\\h_y'\\m_x'\\m_y'\end{pmatrix}=\frac{1}{K}\left[K_x\begin{pmatrix}h_x\\h_y\\m_x\\m_y\end{pmatrix}+K_y\begin{pmatrix}h_y\\-h_x\\m_y\\-m_x\end{pmatrix}\right]. \tag{2.17}$$

The solution of (2.15) is very simple in matrix form,

$$\vec{f}(r)=\cosh r\hat{C}\,\vec{f}_c+\sinh r\hat{C}\,\vec{f}_s \tag{2.18}$$

where $\vec{f}_c$ and $\vec{f}_s$ are constant vectors whose components are determined by the boundary conditions. The construction of the *matrices* $\cosh r\hat{C}$ and $\sinh r\hat{C}$ will be discussed in a later section.

III. SPIN-WAVE MODES

In this section we derive the frequency-versus-wave-vector dispersion relations for a metallic or insulating ferromagnetic plate.

A. Boundary Conditions

The usual boundary conditions must be imposed on the fields. This requires that h_x and h_y and h_z be continuous across the surfaces. We consider two cases in which the boundary conditions are symmetrical. In the first case, the eigenvalue problem, the sample is not driven and the fields *outside* the sample may be derived from a scalar potential $\phi^{(0)}$:

$$\phi^{(0)}=e^{i\vec{k}_{\parallel}\cdot\vec{\rho}}e^{-k_{\parallel}|z|},\qquad \vec{h}^{(0)}=\nabla\phi^{(0)}. \tag{3.1}$$

In the second case the sample is driven by a uniform rf magnetic field $\vec{h}_{rf}$. The fields outside the sample are then $\vec{h}^{(0)}+\vec{h}_{rf}$. In addition we must specify boundary condition on the magnetization at the surface. We shall treat in detail the case for which the spins are "pinned" so that $m_x=m_y=0$ at both surfaces.

For the eigenvalue problem the fields outside decay exponentially as $|z|\to\infty$. According to Eq. (3.1), at $z=\pm d/2$,

$$\delta h_x=iK_x\phi^{(0)},\quad \delta h_y=iK_y\phi^{(0)},\quad \delta h_z=\pm K\phi^{(0)}. \tag{3.2}$$

The boundary conditions may be expressed in terms of the primed fields using Eqs. (2.17) and (2.6) so that the new boundary conditions at $z=\pm d/2$ are

$$\left(1\pm\frac{\epsilon K}{g^2}\frac{\partial}{\partial r}\right)h_x'=0,\quad h_y'=0. \tag{3.3}$$

For the cases of pinned spins the rf magnetization vanishes at the surfaces, $m_x'=m_y'=0$ at $\pm d/2$. When the boundary conditions are symmetric, as we have assumed here, then the solutions are "odd" or "even". In this case the boundary conditions at $\pm d/2$ are redundant and we need only impose them at one surface. We shall use the boundar conditions at $z=d/2$. They may be expressed in matrix form

$$\left(\hat{1}+\frac{\epsilon K}{g^2}\hat{1}_{11}\frac{\partial}{\partial r}\right)\vec{f}'\Big|_{z=d/2}=0, \tag{3.4}$$

where the $\hat{1}_{11}$ matrix elements are zero except for the 1,1 element which is unity. Using Eq. (2.18) we obtain

$$\left(1+\frac{\epsilon K}{g^2}\hat{1}_{11}\hat{C}\tanh r\hat{C}\right)\cosh r\hat{C}\,\vec{f}_c\Big|_{z=d/2}=0 \tag{3.5}$$

and

$$\left(1+\frac{\epsilon K}{g^2}\hat{1}_{11}\hat{C}\coth\gamma\hat{C}\right)\sinh\gamma\hat{C}\,\vec{f}_s\Big|_{z=d/2}=0. \tag{3.6}$$

B. Eigenvalue Problem

Equations (3.5) or (3.6) can be satisfied provided the determinant of the matrix vanishes. This yields the eigenvalue conditions[17]

$$\frac{g^2}{\epsilon K}+\{\hat{C}\tanh r_s\hat{C}\}_{11}=0 \tag{3.7}$$

for the odd modes and

$$\frac{g^2}{\epsilon K}+\{\hat{C}\coth r_s\hat{C}\}_{11}=0 \tag{3.8}$$

for the even modes. In Eqs. (3.7) and (3.8), $\{\ \}_{11}$ indicates the 1, 1 element of the matrix product enclosed and r_s is the value of r evaluated at $z=d/2$.

C. Representation of Matrix Elements

The frequency versus wave-vector k dispersion of the spin-wave modes is determined from Eqs. (3.7) and (3.8). In order to determine the dispersion we need to calculate the matrix elements $\{\hat{C}\tanh\gamma_s\hat{C}\}_{11}$ and $\{\hat{C}\coth\gamma_s\hat{C}\}_{11}$. A convenient method for constructing these matrices is a partial fractions representation. We make use of the expansions

$$\hat{C}\tanh r_s\hat{C}=\frac{2}{r_s}\sum_{\substack{n=1\\(\text{odd})}}^{\infty}\hat{C}^2(\hat{C}^2+\lambda_n\hat{1})^{-1}\ , \tag{3.9}$$

$$\hat{C}\coth r_s\hat{C}=\frac{1}{r_s}+\frac{2}{r_s}\sum_{\substack{n=2\\(\text{even})}}^{\infty}\hat{C}^2(\hat{C}^2+\lambda_n\hat{1})^{-1}\ , \tag{3.10}$$

where

$$\lambda_n=n^2\pi^2(D/4\pi)(1/d)^2 \tag{3.11}$$

and the notation (odd) and (even) in Eqs. (3.9) and (3.10) indicates a sum on the odd or even integers. One advantage of these representations is that they involve only the matrix $\hat{C}^2$ and not $\hat{C}$. The $\hat{C}^2$ matrix is given by Eq. (2.16). One finds that

$$\{\hat{C}\tanh r_s\hat{C}\}_{11}=\frac{2}{r_s}\sum_{\substack{n=1\\(\text{odd})}}^{\infty}\frac{g^2(M_{11}^n+M_{13}^n)}{(g^2+\lambda_n)M_{11}^n+g^2M_{13}^n}\ , \tag{3.12}$$

where

$$M_{11}^n=(g^2+\lambda_n)\left[(\Omega_k'+\lambda_n)^2-\Omega'^2\right]+\alpha(\Omega_k'+\lambda_n) \tag{3.13}$$

and

$$M_{13}^n=(g^2+\lambda_n)(\Omega_k'+\lambda_n)+\alpha\ . \tag{3.14}$$

Further we have that

$$\{\hat{C}\coth r_s\hat{C}\}_{11}=\frac{1}{r_s}+\frac{2}{r_s}\sum_{\substack{n=2\\(\text{even})}}^{\infty}\frac{g^2(M_{11}^n+M_{13}^n)}{(g^2+\lambda_n)M_{11}^n+g^2M_{13}^n}\ . \tag{3.15}$$

D. $k_\parallel = 0$ Spin-Wave Modes in a Metal

As $k_\parallel\to 0, K\to 0$ but $g^2\to\alpha$ and therefore the first term of Eqs. (3.7) or (3.8) becomes arbitrarily large. In order to have solutions of the eigenvalue equations the second terms must be arbitrarily large. Thus the $k_\parallel=0$ spin-wave eigenvalues are at the poles of the functions $\{\hat{C}\tanh r_s\hat{C}\}_{11}$ and $\{\hat{C}\coth r_s\hat{C}\}_{11}$. Using Eqs. (3.12) and (3.13) we find that the $K=0$ poles are determined by

$$(\alpha+\lambda_n)M_{11}^n+\alpha M_{13}^n=0\ , \tag{3.16}$$

where n is any nonzero positive integer. This equation is easily solved for the eigenfrequencies $\Omega_n(0)$ using Eqs. (3.13) and (3.14). We find that

$$\Omega_n(0)=\{\omega_n+2i[2i+n^2\pi^2(\delta/d)^2]^{-1}\}(1+il)\ ,$$
$$\omega_n=\Omega_H+\lambda_n\ . \tag{3.17}$$

Each standing spin-wave frequency consists of an exchange contribution λ_n, an internal field contribution Ω_H, and a dipolar contribution. The factor $(1+il)$ accounts for the magnetic (phenomenological damping) losses. This loss is proportional to the frequency.

The real part of the frequency,

$$\Omega_{nR}(0)=\omega_n+[4-2ln^2\pi^2(\delta/d)^2]\{4+[n^2\pi^2(\delta/d)^2]^2\}^{-1} \tag{3.18}$$

is the frequency for spin-wave resonance. The imaginary part of $\Omega_n(0)$ is

$$\Omega_{nI}(0)=l\omega_n+2[n^2\pi^2(\delta/d)^2+2l]\{4+[n^2\pi^2(\delta/d)^2]^2\}^{-1}\ , \tag{3.19}$$

which is the spin-wave linewidth due to phenomenological damping and eddy-current losses. The linewidth as measured in a FMR experiment is discussed in Sec. V. The term $\Omega_{nI}(0)$ is a measure of the linewidth. We note that the eddy-current contribution [i.e., $\Omega_{nI}(0)$ for $l=0$] is largest for the low-frequency modes (small n), while the pure-magnetic-loss contribution $l\omega_n$ increases with n. In addition, there is a contribution to $\Omega_{nI}(0)$ involving both eddy-current losses and magnetic losses which is largest for the low-lying modes.

The general behavior of the real part of the frequency is not simple. When $d\ll\delta$ the frequency is dominated by the exchange contribution and $\Omega_{nR}(0)\approx\omega_n$. In this limit the spin-wave modes are ordered with the frequency increasing monotonically with n. In this case the linewidth is dominated by magnetic losses.

If $d\gg\delta$ then the magnetostatic energy dominates the exchange energy and the spin-wave mode ordering is inverted with the lowest modes near Ω_H+1. As n increases the frequency tends towards Ω_H. Finally when n is very large the exchange energy becomes dominant and the frequency begins to increase with n. These features are shown schematically in Fig. 1. The minimum frequency or turning point Ω_t becomes independent of thickness for large thickness. The minimum of $\Omega_{nR}(0)$ with respect to n calculated from Eq. (3.18) is

$$\Omega\approx\Omega_H+\epsilon^{4/3}[3\sqrt{6}+(\tfrac{4}{3})^{2/3}]-\frac{2l}{3\sqrt{6}}\epsilon^{2/3} \tag{3.20}$$

provided that $l\ll\epsilon^{2/3}$. For Permalloy ϵ ranges

from 10^{-2} to 10^{-3} at microwave frequencies. In good quality samples l is of the order of 10^{-3} so that the inequality $l \ll \epsilon^{2/3}$ is usually satisfied. In thick samples Ω_t is an accumulation point for the spin-wave frequencies. The effect of this large density of modes in the microwave power absorption spectrum is masked by the large "exchange shift" absorption peak (discussed in Sec. V).

E. Insulator Spin-Wave Modes

Next we derive the general expressions for the spin-wave eigenvalues of an insulating ferromagnet. The eigenvalue equations can be obtained from Eqs. (3.7) and (3.8) in the insulator limit ($\delta \to \infty$) but some care must be exercised. In this limit $g^2 \to \Omega_{ex} \equiv (D/4\pi)k_\parallel^2$ and $\epsilon K/g^2 \to (D/4\pi)^{-1/2}k_\parallel^{-1}$. The eigenvalue equations are

$$\frac{1}{(D/4\pi)^{1/2}k_\parallel} + \frac{4(D/4\pi)^{1/2}}{d} \sum_{\substack{n=1 \\ (\text{odd})}}^{\infty} A_n = 0 \qquad (3.21)$$

for the odd modes and

$$\frac{1}{(D/4\pi)^{1/2}k_\parallel} + \frac{2}{d(D/4\pi)^{1/2}k_\parallel^2} + \frac{4(D/4\pi)^{1/2}}{d} \sum_{\substack{n=2 \\ (\text{even})}}^{\infty} A_n \qquad (3.22)$$

for the even modes, where

$$A_n = \frac{(\Omega_k' + \lambda_n)^2 - \Omega'^2 + (\Omega_k' + \lambda_n)}{(\Omega_{ex} + \lambda_n)[(\Omega_k' + \lambda_n)^2 - \Omega'^2] + \Omega_{ex}(\Omega_k' + \lambda_n)} \ . \qquad (3.23)$$

We see from Eqs. (3.21) and (3.22) that the $k_\parallel = 0$ modes correspond to the poles of A_n. The insulator $k_\parallel = 0$ frequencies are

$$\tilde{\Omega}_n(0) = (\Omega_n + \lambda_n)(1 + il) \ , \qquad (3.24)$$

where the tilde over $\Omega_n(0)$ is used to distinguish the insulator frequencies from the metallic frequencies. In Eq. (3.24) n is any positive, nonzero integer.

The lowest mode is the $n = 1$ mode for which

$$\Omega_1(0) = [\Omega_H + (D/4\pi)\,\pi^2/d]\,(1 + il) \ . \qquad (3.25)$$

The usual magnetostatic branch would have $\Omega_{mag} = \Omega_H$ for $k_\parallel = 0$. In the case that the spins are pinned at the surface, the usual magnetostatic branch does not exist.[18]

F. Metallic Magnetoexchange Branches

In this section we derive expressions for the dispersion of the spin-wave modes for small values of $K = \delta k_\parallel$.

The linear dependence of the spin-wave modes is easily obtained from the eigenvalue equations (3.7) and (3.8). From Eqs. (3.12) and (3.15) we see that linear terms in K do not occur explicitly in the matrix element $(\hat{C}\tanh r_s \hat{C})_{11}$ or $(\hat{C}\coth r_s \hat{C})_{11}$. The eigenvalue equation (to first order in K) is

$$\frac{-i\epsilon r_s}{K} = \sum_{\substack{n=1 \\ (\text{odd})}}^{\infty} \frac{\alpha(M_{11}^n + M_{13}^n)}{(\alpha + \lambda_n)M_{11}^n + \alpha M_{13}^n} \qquad (3.26)$$

for the odd modes and

$$-\left(\frac{i\epsilon r_s}{K} + \frac{1}{2}\right) = \sum_{\substack{n=2 \\ (\text{even})}} \frac{\alpha(M_{11}^n + M_{13}^n)}{(\alpha + \lambda_n)M_{11}^n + \alpha M_{13}^n} \qquad (3.27)$$

for the even modes. For small K solutions of Eqs. (3.26) and (3.27) exist only if at least one of the denominators in the sum is of order K. We suppose that the nth denominator is such that

$$(\alpha + \lambda_n)M_{11}^n + \alpha M_{13}^n = \beta K \ , \qquad (3.28)$$

then from Eq. (3.26) or (3.27) we find that

$$\beta = -\alpha\lambda_n \Omega_n(0)/ir_s\epsilon \ . \qquad (3.29)$$

Writing

$$\Omega_n^2(K) = \Omega_n^2(0) + \Delta(\Omega_n^2) \ , \qquad (3.30)$$

one finds from Eqs. (3.28) and (3.29) that

$$\Delta(\Omega_n^2) = -\beta K/(\alpha + \lambda_n)^2 \ . \qquad (3.31)$$

Finally solving explicitly for the eigenfrequency we obtain

$$\Omega_n(k_\parallel) = \Omega_n(0) + (1 + il)\left(\frac{2n^2\pi^2(\delta/d)^4}{[2i + n^2\pi^2(\delta/d)^2]^2}\right) k_\parallel d \ . \qquad (3.32)$$

The last term is the magnetostatic or dipolar dispersion of the metallic spin-wave modes. This contribution also contains both magnetic and eddy-current losses.

Equation (3.32) is valid if $\delta k_\parallel \ll 1$ and only one denominator is of the order of K. The latter condition requires that the spacing between the $K = 0$ frequencies be much larger than the dipolar dispersion. This leads to the condition

$$k_\parallel d \ll \frac{2\lambda_n}{n}\left(\frac{[2i + n^2\pi^2(\delta/d)^2]^2}{2n^2\pi^2(\delta/d)^4}\right) \ . \qquad (3.33)$$

For large n values this reduces to the requirement that $k_\parallel d \ll n(D/4\pi)(\pi/d)^2$.

G. Insulator Magnetoexchange Branches

The same procedure used in the preceding section may be applied to Eqs. (3.22) and (3.23) to obtain the spin-wave dispersion of the insulator spin-wave modes. In this case it is important to note that the odd and even modes have qualitatively different dispersions. For small $k_\parallel$ the odd mode solutions, according to Eq. (3.22), are controlled by a term linear in $1/k_\parallel$. According to Eq. (3.23) the controlling term for the even modes is quadratic in $1/k_\parallel$. As a consequence, the odd modes will have a linear dispersion in $k_\parallel$ while the even-mode dispersion is quadratic in $k_\parallel$.

The results are that

$$\tilde{\Omega}_n(K) = \Omega_H\left[\Omega_H + \lambda_n + \left(\frac{2}{n^2\pi^2}\right)k_\parallel d\right](1 + il) \qquad (3.34)$$

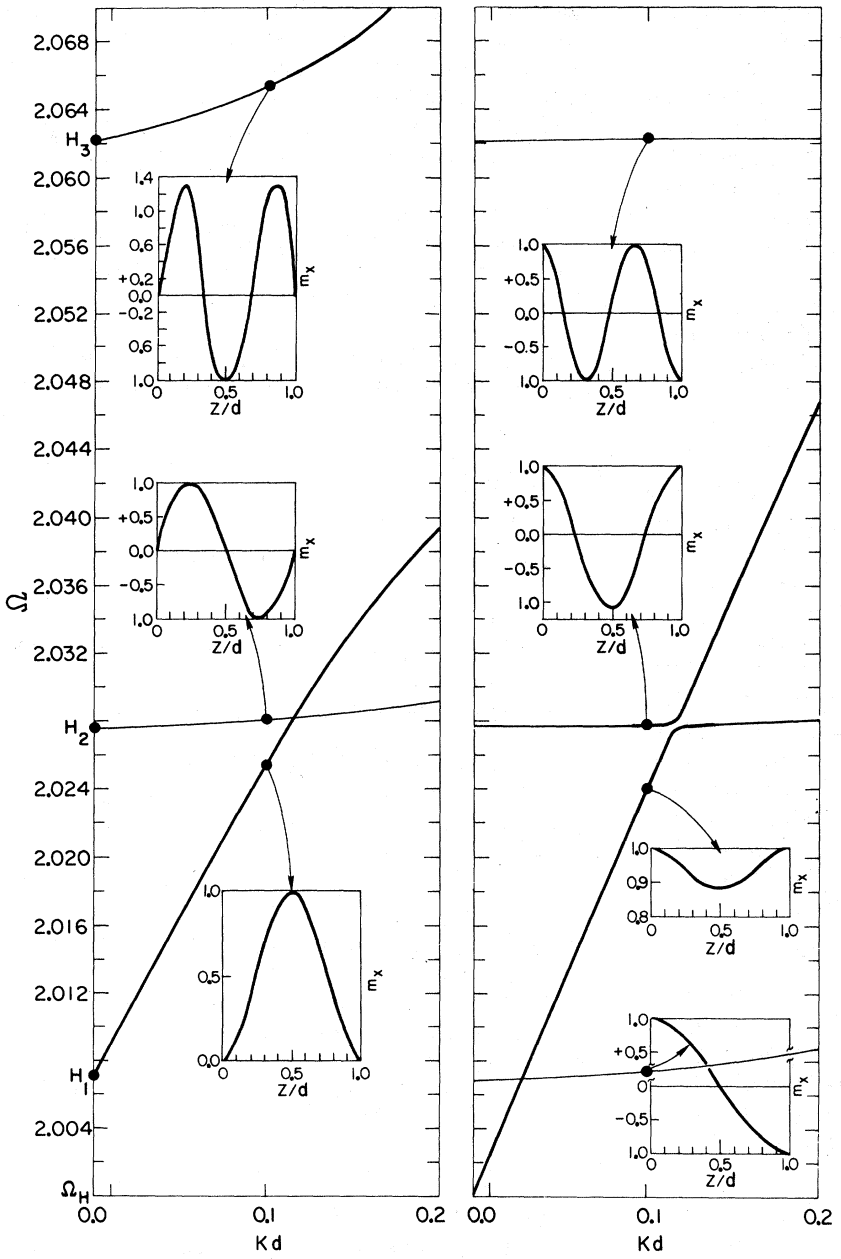

FIG. 2. Numerical calculation of the magnetoexchange branches of a thin insulating film with pinned (left) and unpinned (right) boundary conditions. The heavy solid line on the right rising linearly from $\Omega = \Omega_H$ is the magnetostatic branch for the unpinned case. The horizontal branches are standing spin-wave branches. The inserts are graphs of the distribution of magnetization at the indicated frequencies. The left-hand graph shows the spectrum for the same insulating film with pinned boundary conditions. The heavy solid curve is the lowest magnetoexchange branch. The first, third, . . . branches initially have linear slopes while the even-numbered branches are quadratic. The first branch has a slope of $2/\pi^2 \approx 0.2$. The slope of the magnetostatic branch is 1/4. The parameters used are $d = 0.61\times10^{-4}$ cm, $D/4\pi = 2.6\times10^{-12}$ cm^2, $4\pi M_s = 1750$ Oe, and $l = 0$.

for $n = 1, 3, 5 \ldots$ and

$$\tilde{\Omega}_n(k) = \left[\Omega_H + \Omega_{ex} + \lambda_n + \frac{3}{2}\frac{(k_\parallel d)^2}{n^2\pi^2}\right](1 + il) \qquad (3.35)$$

for $n = 2, 4, 6 \ldots$.

The term linear in $k_\parallel$ in the odd-mode frequencies and the quadratic term $\frac{3}{2}(k_\parallel d)/n^2\pi^2$ in the even-mode frequencies are due to dipolar effects. The term $\Omega_{ex} + \lambda_n$ is the total exchange energy associated with the even modes. Equations (3.33) and (3.34) are valid if $k_\parallel d \ll 1$ and the mode spacing is large compared to the dispersion. This requires that $\pi^2 n\lambda_n \gg k_\parallel d$. The character of these modes is illustrated in Fig. 2 for a YIG film with a thickness $d = 0.61\times10^{-4}$ cm. The dispersion curves in Fig. 2 were obtained by numerical solution of the exact eigenvalue equation. The parameters used were $D/4\pi = 2.6\times10^{-12}$, $4\pi M_s = 1750$ Oe, and $\vec{l} = 0$. The linear dispersion of the odd levels and the quadratic dispersion of the even levels for small $k_\parallel d$ confirms the expressions derived here.

For comparison, the spectrum for the unpinned case ($\partial m_x/\partial z$ and $\partial m_y/\partial z$ vanish at the surfaces) is also shown in the right-hand figure of Fig. 2. The heavy approximately linear curve rising from $\Omega = \Omega_H$ is the magnetostatic branch frequently ob-

served for insulators. This branch has a slope of $\frac{1}{4}$. In contrast, the left-hand figure of Fig. 2 for the pinned boundary conditions does not have a branch starting from Ω_H. The lowest branch begins at $\Omega = \Omega_H + (D/4\pi)(\pi/d)^2 = H_1$. The initial slope of $2/\pi^2$ is about 20% lower than that of the magnetostatic branch. The linearity of the lowest (pinned) magnetoexchange branch is destroyed by the strong interaction with the third magnetoexchange branch which starts at $H_3 = \Omega_H + 9(D/4\pi)(\pi/d)^2$.

A discussion of the insulator modes for the pinned and unpinned boundary conditions for perpendicular resonance and also for parallel resonance has been given elsewhere.[18]

IV. MICROWAVE POWER ABSORPTION SPECTRUM

In this section we calculate Poynting's vector for a metallic ferromagnetic plate driven by a uniform h_{rf}. The power absorbed by the specimen is proportional to the normal component of Poynting vector integrated over the entire surface. Our development differs from the usual calculation of the surface impedance in a number of respects. First, we develop expressions which are valid for $k_{\parallel} \neq 0$. Second, we present a very detailed analysis of the $k_{\parallel} = 0$ absorption spectrum. Simple analytical formulas are derived which describe the standing spin-wave resonances absorption peaks and the derivatives of the absorption peaks with an accuracy of a few percent including the effects of magnetic damping, exchange, and eddy currents.

A. Response to a Uniform Field

If the effects of displacement currents are neglected then the response of the sample to a uniform rf magnetic field $\vec{h}_{rf}(t) = \exp(i\omega t)\vec{h}_{rf}$ may be easily calculated by modifying the boundary conditions. Let us assume that h_{rf} is linearly polarized along the x' axis so that the boundary condition of Eq. (3.3) becomes

$$\left(1 \pm \frac{\epsilon K}{g^2}\frac{\partial}{\partial r}\right) h_x' = h_{rf}\,, \qquad h_y' = m_x' = m_y' = 0 \tag{4.1}$$

at $z = \pm d/2$. We then obtain from Eq. (2.15) the matrix equation

$$\left(\hat{1} \pm \frac{\epsilon K}{g^2}\hat{1}_{11}\frac{\partial}{\partial r}\right) f'|_{z=\pm d/2} = h_{rf}\begin{pmatrix}1\\0\\0\\0\end{pmatrix}\,, \tag{4.2}$$

where the components f' are now the fields generated in response to h_{rf}. Since the driving field is symmetric about $z = 0$ the sample modes of response must also by symmetrical. The h field at $\pm\infty$ is h_{rf} rather than zero as in the eigenvalue problem. As a result only the cosh-type solutions can satisfy Eq. (4.2). When $k_{\parallel} = 0$ this is simply the statement that modes having an integral number of wavelengths across a ferromagnetic film are not excited by a uniform rf field. By using $\vec{f}' = (\cosh r\hat{C})\vec{f}_R$ we find the response amplitude inside the sample at the surfaces $\pm d/2$ is given by

$$\vec{f}_R\left(\frac{d}{2}\right) = h_{rf}(\cosh r_s\hat{C})^{-1}\left(\hat{1} + \frac{\epsilon K}{g^2}\hat{1}_{11}\hat{C}\tanh r_s\hat{C}\right)^{-1}\begin{pmatrix}1\\0\\0\\0\end{pmatrix}. \tag{4.3}$$

The fields $(h_x')^*$ and $(\partial/\partial r)h_x'$ will be needed for the calculation of the power absorbed by the sample. They are

$$\left[h_x'\left(\frac{d}{2}\right)\right]^* = h_{rf}^*\left[\left(\hat{1} + \frac{\epsilon K}{g^2}\hat{1}_{11}\hat{C}\tanh r_s\hat{C}\right)^{-1}\right]^*_{11} \tag{4.4}$$

and

$$\frac{\partial}{\partial r}h_x'\left(\frac{d}{2}\right) = h_{rf}\left[(\hat{C}\,\mathrm{Tanh} r_s\hat{C})\left(\hat{1} + \frac{\epsilon K}{g^2}\hat{1}_{11}\hat{C}\tanh r_s\hat{C}\right)^{-1}\right]_{11}\,.$$

The elements of the inverse matrix are

$$\left(\hat{1} + \frac{\epsilon K}{g^2}1_{11}\hat{C}\tanh r_s\hat{C}\right)^{-1} = \begin{pmatrix} \frac{1}{1+T_{11}} & \frac{-T_{12}}{1+T_{11}} & \frac{-T_{13}}{1+T_{11}} & \frac{-T_{14}}{1+T_{11}} \\ 0 & 1 & 0 & 0 \\ 0 & 0 & 1 & 0 \\ 0 & 0 & 0 & 1 \end{pmatrix}, \tag{4.5}$$

where

$$T_{ij} = \frac{\epsilon K}{g^2}\{\hat{C}\tanh r_s\hat{C}\}_{ij}\,. \tag{4.6}$$

Using this result we find that

$$\left[h_x'\left(\frac{d}{2}\right)\right]^* = h_{rf}^*\left[(1+T_{11})^{-1}\right]^*\,, \qquad \frac{\partial}{\partial r}h_x'\left(\frac{d}{2}\right) = h_{rf}\,T_{11}\,\frac{g^2}{\epsilon K}(1+T_{11})^{-1}\,. \tag{4.7}$$

B. Power Absorption

The power absorbed by the sample can be calculated from Poynting's theorem[19] which states that the power flow P per unit surface area into a region (averaged over a cycle) is given by

$$P = \frac{1}{2S}\,\mathrm{Re}\left(\int_{\mathrm{surf}}(\vec{e}\times\vec{h}^*)\cdot\vec{n}\,ds\right)\,. \tag{4.8}$$

In Eq. (4.8) the integral is over the entire bounding surface whose *inward* unit normal is $\vec{n}$ and whose surface area is S. For our planar geometry Poynt-

ing's vector $\vec{e}\times\vec{h}^*$ is uniform on each surface and changes sign on going from $z=+d$ to $z=-d$. Since $\vec{n}$ also changes sign we find that the power absorbed by the sample is

$$P_\perp = -\,\mathrm{Re}(\vec{e}\times\vec{h}^*)_z\big|_{z=d/2}\,, \tag{4.9}$$

since $\vec{e}\times\vec{h}^* = \vec{e}'\times(\vec{h}')^*$ and $h_y'=0$ at $z=d/2$. The expression for $P_\perp$ reduces to

$$P_\perp = \frac{c}{4\pi\sigma}\,\mathrm{Re}\left(\frac{2i\epsilon}{\delta g^2}\,h_x'^*\,\frac{\partial}{\partial r}\,h_x'\right)\Bigg|_{z=d/2}\,. \tag{4.10}$$

It is convenient to define a generalized complex surface impedance $Z(\omega, k_\parallel)$ by the relation

$$Z(\omega,k_\parallel) = \frac{2i\epsilon}{g^2\,|h_{rf}|^2}\left(h_x'^*\,\frac{\partial}{\partial r}\,h_x'\right)\Bigg|_{z=d/2}\,. \tag{4.11}$$

The function reduces to the usual surface impedance function when $k_\parallel=0$. The power absorbed per unit area divided by $|h_{rf}|^2$ averaged over a cycle is given by

$$P_\perp(\omega,k_\parallel) = \frac{c}{(4\pi\sigma)\delta}\,\mathrm{Re}[Z(\omega,k_\parallel)]\,. \tag{4.12}$$

Now we can make use of Eq. (4.7) to derive the result

$$Z(\omega,k_\parallel) = \frac{+2i}{K}\,\frac{T_{11}}{|1+T_{11}|^2}\,. \tag{4.13}$$

The function $T_{11} = (\epsilon K/g^2)\{\hat{C}\tanh r_s\hat{C}\}_{11}$ may be calculated by using Eq. (3.12).

C. Trigonometric Representation of T_{11} at $k_\parallel=0$

It is informative to have a representation of T_{11} in terms of the propagation vectors in the ferromagnetic medium. Such a representation can be obtained by diagonalizing the matrix $\hat{C}^2$ and then constructing the matrix $\hat{C}\tanh r_s\hat{C}$ in terms of the eigenvalues of $\hat{C}$. The eigenvalues c_i of $\hat{C}$ are related to the propagation vectors in the medium $k_{\perp i}$ by the relation

$$(D/4\pi)k_{\perp i}^2 = -\,c_i \quad (i=1,\,2,\,3,\text{ and }4)\,. \tag{4.14}$$

An alternate procedure is to resolve each term of Eq. (3.12) into a sum of terms by finding the roots of the denominator. The individual factors may be summed to produce trigonometric functions of the $k_{\perp i}$. The details of such procedures will not be presented here. The result for $k_\parallel=0$ is

$$Z(\omega,k_\parallel=0) = Z^{(+)} + Z^{(-)}\,,$$
$$Z^{(\pm)} = \frac{k_1^{(\pm)}\tan k_1^{(\pm)}d/2 - k_2^{(\pm)}\tan k_2^{(\pm)}d/2 + (i\delta^2/2)k_1^{(\pm)}k_2^{(\pm)}(k_2^{(\pm)}\tan k_1^{(\pm)}d/2 - k_1^{(\pm)}\tan k_2^{(\pm)}d/2)}{i\delta[(k_1^{(\pm)})^2 - (k_2^{(\pm)})^2]} \tag{4.15}$$

The quantities $k_1^{(\pm)}$ and $k_2^{(\pm)}$ [denoted by $k_{\perp i}$ in Eq. (4.14)] are the propagation constants for the ferromagnetic metal

$$\frac{D}{4\pi}\,(k_{1,2}^{(+)})^2 = \left(\frac{\eta-\alpha}{2}\right) \pm \left[\left(\frac{\eta-\alpha}{2}\right)^2 + (\eta-1)\alpha\right]^{1/2}\,, \tag{4.16}$$

where $\eta=\Omega'-\Omega_H'$, $\Omega_H'=\Omega_H+i\Omega'$, and $\alpha=2i\epsilon^2$. The quantities $k_{1,2}^{(-)}$ may be obtained from Eq. (4.16) using $\eta=\Omega'+\Omega_H'$. The quantities with the (+) symbol correspond to right-hand circularly polarized waves and the (−) quantities to left-hand circularly polarized waves. Since our source field $\vec{h}_{rf}$ is linearly polarized the system response is the sum of the two circularly polarized responses. An expression for T_{11}^+ similar to Eq. (4.5) was derived and discussed by Pincus.[9]

V. CHARACTERISTICS OF THE POWER ABSORPTION SPECTRUM

The microwave power absorption spectrum may be qualitatively described as consisting of a smooth ferromagnetic resonance background (FMRB) which is peaked at $\Omega_H \approx \Omega + 2\epsilon$ plus a series of spin-wave resonance peaks (SWRP). The theoretical power absorption spectrum for a 5000-Å Permalloy film is shown in Fig. 3 for several values of the magnetic-loss parameter l. In metallic ferromagnetic films the amplitude of the FMRB increases relative to the amplitude of the SWRP as the sample thickness increases. In films whose thickness $d \ll \delta$ the amplitudes of the SWRP are large compared to the FMRB amplitude, while for $d \gg \delta$ the converse is true.

The FMRB is principally due to eddy-current losses. The magnetic losses (phenomenological damping) also contribute to the background and broaden and diminish the SWRP. The peak in the FMRB is due to the large increase in the magnetic susceptibility of the ferromagnetic medium near $\Omega=\Omega_H$. In fact, in the absence of the exchange interaction, the susceptibility and hence the power absorption would be infinite at $\Omega=\Omega_H$. Ament and Rado[4,5] and Pincus[9] showed that the effect of exchange was to shift the FMR peak by an amount proportional to $\epsilon=(D/4\pi\delta^2)^{1/2}$. This "exchange shift" has been used to determine the exchange stiffness in thick samples. The amplitude of the FMR peak is proportional to ϵ^{-1}. When magnetic losses are considered both the exchange shift and the peak height are changed. When $\Omega l \gg \epsilon$, the features are governed by Ωl rather than ϵ. The FMR

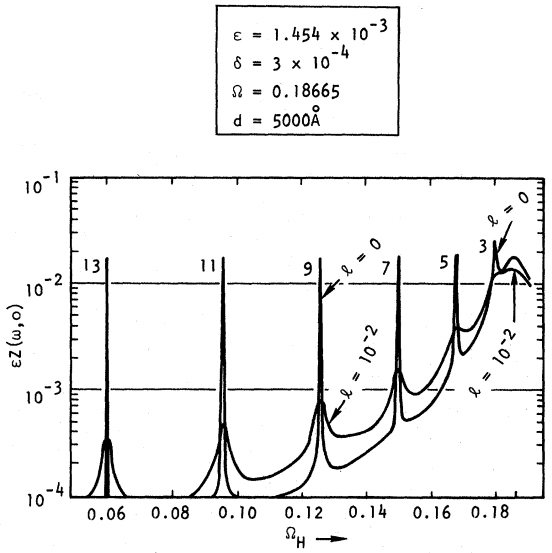

FIG. 3. The $k_{\parallel}=0$ surface impedance for a 5×10^{3}-Å Permalloy film as a function of l the phenomenological relaxation parameter. When $l=0$ the peak height of the spin-wave resonance is the same for all of the standing spin-wave modes. The odd spin-wave modes 3–13 are labeled with the appropriate number. The $n=1$ resonance is obscured by the ferromagnetic resonance peak. When $l\neq0$ the peak height of the higher modes decreases as $1/n^2$. The parameter $\Omega=0.18665$ corresponds to a frequency of 6 GHz.

peak also depends upon $k_{\parallel}$. The peak shifts to higher frequencies (or lower Ω_H for fixed Ω) as $k_{\parallel}$ increases. For $(D/4\pi)k_{\parallel}^2\ll1$ the $k_{\parallel}$ dispersion of the FMR peak is due to dipolar effects. We shall refer to this dispersion as "dipolar dispersion." The SWRP also show dipolar dispersion as discussed in Sec. III G. When $d\gg\delta$ the SWRP cannot be resolved and only the FMRB is evident. The dipolar dispersion of the FMR peak depends upon $\delta k_{\parallel}$ and hence for $d>\delta$ is independent of the sample thickness. This is in sharp contrast to the behavior of the magnetostatic dispersion of the main resonance in an insulating ferromagnet where the dispersion depends upon $k_{\parallel}d$. The SWRP in the metal and insulator also depend upon $k_{\parallel}d$ [see Eqs. (3.32)–(3.34)]. However, in the metal when $d\gg\delta$ the SWRP cannot be resolved because the mode spacing is smaller than the eddy-current linewidth and the FMRB is much larger than the amplitude of the SWRP.

Another important feature of the absorption spectra is the "antiresonance"[2] which occurs at $\Omega_H=\Omega-1$ ($\gamma H_{app}=\omega$). The antiresonance is a minimum in the FMRB. In the case of perpendicular resonance, this minimum is associated with the right-hand circularly polarized component. The nature of the antiresonance is shown in Fig. 4. It is evident that the antiresonance is produced by the absence of absorption of the right-hand circularly component of the rf field. The type of effect has also been observed in recent ferromagnetic transmission experiments[15] in which maximum transmission of microwave energy through a sample occurs at $\Omega_H=\Omega-1$.

In this section we shall extract these features from the theoretical results derived in the preceding sections. We derive simple and convenient approximate expressions for the absorption spectrum and also for the derivative of this function since this is the quantity frequently measured in resonance experiments.

A. Ferromagnetic Resonance Background

It is evident from Fig. 3 that the power absorption spectrum consists approximately of a background which increases as $(\Omega-\Omega_H)^{-1}$ [provided $(\Omega-\Omega_H)\gg\epsilon=1.454\times10^{-3}$]. The origin of this effect can be seen from Eq. (4.16). When $1\gg\eta\gg|\alpha|=2\epsilon^2$, then

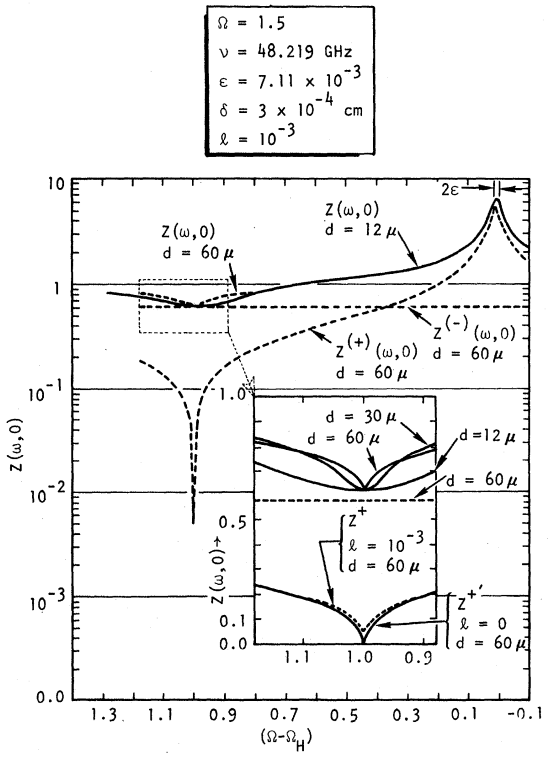

FIG. 4. The $k_{\parallel}=0$ surface impedance for thick films showing both the ferromagnetic resonance peak ($\Omega-\Omega_H=2\epsilon$) and the antiresonance ($\Omega-\Omega_H=1.0$). The heavy line is the total surface impedance ($Z=Z^{(+)}+Z^{(-)}$) and the dashed lines are the right- ($Z^{(+)}$) and left-hand ($Z^{(-)}$) circular polarization contributions. The resonance peak (antiresonance) is associated with a maximum (minimum) in $Z^{(+)}$. $Z^{(-)}$ is approximately constant. The insert shows the dependence of the antiresonance on the thickness. The 60-μ heavy curve is the sum of the two dashed curves.

$$(k_1^{\pm})^2 \approx \frac{\pm\Omega' - \Omega_H'}{D/4\pi}, \tag{5.1}$$

$$(k_2^{\pm})^2 \approx \left(\frac{1}{\pm\Omega' - \Omega_H'} - 1\right)\frac{2i}{\delta^2} \quad . \tag{5.2}$$

The quantity k_1^+ corresponds to the exchange wave while k_2^+ is the wave vector for the eddy-current wave. We note that $k_1^{\pm}$ is very large compared to $k_2^{\pm}$ since $D/4\pi \sim 10^{-12}$ to 10^{-14} cm^{-2} while $\delta^2 \sim 10^{-7}$ cm^{-2}. We use this fact to derive from Eq. (4.15) the approximate relation

$$Z_{\mathrm{FMRB}} \approx \frac{-\delta}{2}\left(k_2^+ \tan k_2^+ \frac{d}{2} + k_2^- \tan k_2^- \frac{d}{2}\right), \tag{5.3}$$

where $k_2^{\pm}$ is given by Eq. (5.2).

In deriving Eq. (5.3) we have neglected terms of the form $(\tan k_1^+ d/2)/k_1^+$. These terms are not small when $k_1^+ d/2 \to (2n+1)\pi$ since then $\tan(k_1^+ d/2) \to \infty$. The exact expression for $k_1^{\pm}$ contains an imaginary part so that $\tan k_1 d/2$ is always finite. However, in neglecting these terms we have eliminated the SWRP. Thus the expression derived represents the FMRB due to eddy currents. It follows from Eq. (5.2) that $|k_2^{\pm}| \sim 1/\delta$ so that if $d \ll \delta$ we may approximate $\tan(k_1^{\pm} d/2)$ by the first terms of its power series expansion. In this way we find that

$$Z_{\mathrm{FMRB}}(\omega, k_{11}=0)$$

$$\equiv \mathrm{Re}[Z_{\mathrm{FMRB}}(\omega, k_{11}=0)] \approx \mathrm{Re}\left(\frac{\delta d^3}{48}(k_1^+)^4 + (k_2^-)^4\right)$$

$$\approx \frac{(d/\delta)^3}{12}\left\{\left(\frac{1}{\Omega - \Omega_H} - 1\right)^2 + \left(\frac{1}{\Omega + \Omega_H} + 1\right)^2\right\}. \tag{5.4}$$

This equation is valid only when $(\Omega - \Omega_H) \gg \epsilon$. Therefore, the FMR peak is not described by this result. As we commented earlier the FMR peak is controlled by the exchange interaction and not by the eddy currents. However, we shall show later that when $\Omega l \gg \epsilon$ then the peak is controlled by magnetic losses. In this case Eq. (5.3) is valid when Eq. (5.2) is used for the propagation constants. Note that $\Omega_H' = \Omega_H + i\Omega l/(1+l^2)$ enters in Eq. (5.3) and not simply Ω_H.

B. Spin-Wave Resonance Peaks

Next we derive approximate expressions for the SWRP contribution to the power absorption spectrum.

When $d \ll \delta$ it is easily verified that the major contribution to $T_{11}\{\hat{C}\coth r_s \hat{C}\}_{11}$ comes from a single term in the partial fractions expansion of Eq. (3.12). From Eq. (3.18) we see that the nth spin-wave resonance occurs at an applied field $\Omega_H \approx \Omega - \lambda_n$ when $d \ll \delta$.

For Ω_H near $\Omega - \lambda_n$ the expression for the surface impedance is

$$Z_{\mathrm{SWRP}}^n \approx 4\left(\frac{\delta}{d}\right)\frac{\alpha(M_{11}^n + M_{13}^n)}{(\alpha+\lambda_n)M_{11}^n + \alpha M_{13}^n}, \tag{5.5}$$

where $\alpha = 2i\epsilon^2$ and M_{11}^n, M_{13}^n, and λ_n have been defined previously. The neglected terms contribute a background absorption which is approximated by Eq. (5.4). Before proceeding let us establish the magnitude of the various quantities. For a 5000-Å Permalloy film with a skin depth of 3×10^{-4} cm, exchange stiffness $A = 0.9\times10^{-6}$ erg/cm, $4\pi M_s = 10.9\times10^3$ Oe and for a frequency of 6 GHz we find that $\epsilon = 1.454\times10^{-3}$, $\lambda_n = 0.75\times10^{-3}n^2$, $\Omega = 0.18655$, $|\alpha| = 4.2282\times10^{-6}$, and $\delta/d = 6$. We shall assume that the phenomenological damping parameter $l \lesssim 10^{-2}$ or that $1/\tau \lesssim 3\times10^8$ sec^{-1}. Using the inequalities $|\alpha| \ll \lambda_n$, $|\alpha| \ll \Omega$, and $\Omega l \ll \omega_n$, we derive the expression

$$Z_{\mathrm{SWRP}}^n \approx \left(\frac{w}{d}\right)\frac{|\alpha|}{\lambda_n}\Omega\frac{\Gamma_n}{(\omega_n^2 - \Omega^2)^2 + \Gamma_n^2}, \tag{5.6}$$

where

$$\omega_n = \Omega_H + \lambda_n, \quad \Gamma_n = 2\Omega(\Omega l + |\alpha|/\lambda_n). \tag{5.7}$$

This expression is valid for $\lambda_{n+1} - \lambda_n > 2(\Omega_H - \omega_n) > \lambda_n - \lambda_{n-1}$ for each resonance provided $(\Omega - \Omega_H) \gg \epsilon$. We see that the resonance linewidth Γ_n increases with Ω. Since $|\alpha| \propto \Omega$ (because of the skin depth dependence) Γ_n varies as Ω^2.

The total power absorbed is the sum of the two contributions

$$Z_{\mathrm{total}}^n(\omega, k_{11}=0) \approx 4\frac{\delta}{d}\frac{|\alpha|}{\lambda_n}\Omega\frac{\Gamma_n}{(\omega_n^2 - \Omega^2)^2 + \Gamma_n^2} + \frac{(d/\delta)^2}{12}\left[\left(\frac{1}{\Omega - \Omega_H} - 1\right)^2 + \left(\frac{1}{\Omega + \Omega_H} + 1\right)^2\right],$$

$$(\lambda_{n+1} - \lambda_n) > 2(\Omega_H - \omega_n) > (\lambda_n - \lambda_{n-1}) \quad . \tag{5.8}$$

This result is an excellent approximation to the exact expression

$$Z_{\mathrm{total}} = 4\frac{\delta}{d}\alpha\sum_{n=0}\frac{M_{11}^n + M_{13}^n}{(\alpha+\lambda_n)M_{11}^n + \alpha M_{13}^n} \quad . \tag{5.9}$$

In Fig. 5 we illustrate the excellence of Eq. (5.8) in describing the power absorption peaks which are removed from the main FMR (i.e., $n \geq 5$). For perspective the reader should refer to Fig. 3 which shows the entire spectrum calculated from the Eq. (5.9). In Fig. 5, the curves labeled "exact" are calculated from Eq. (5.9) while those marked "approx" are calculated from Eq. (5.8). The agreement can be further improved if Eq. (5.3) is used for the FMRB contribution. For the peak $n = 13$ and $l = 10^{-3}$ the FMRB is only about 2% of the SWRP while for $n = 5$ the two contributions are about the same magnitude. As l increases the FMRB is relatively more important.

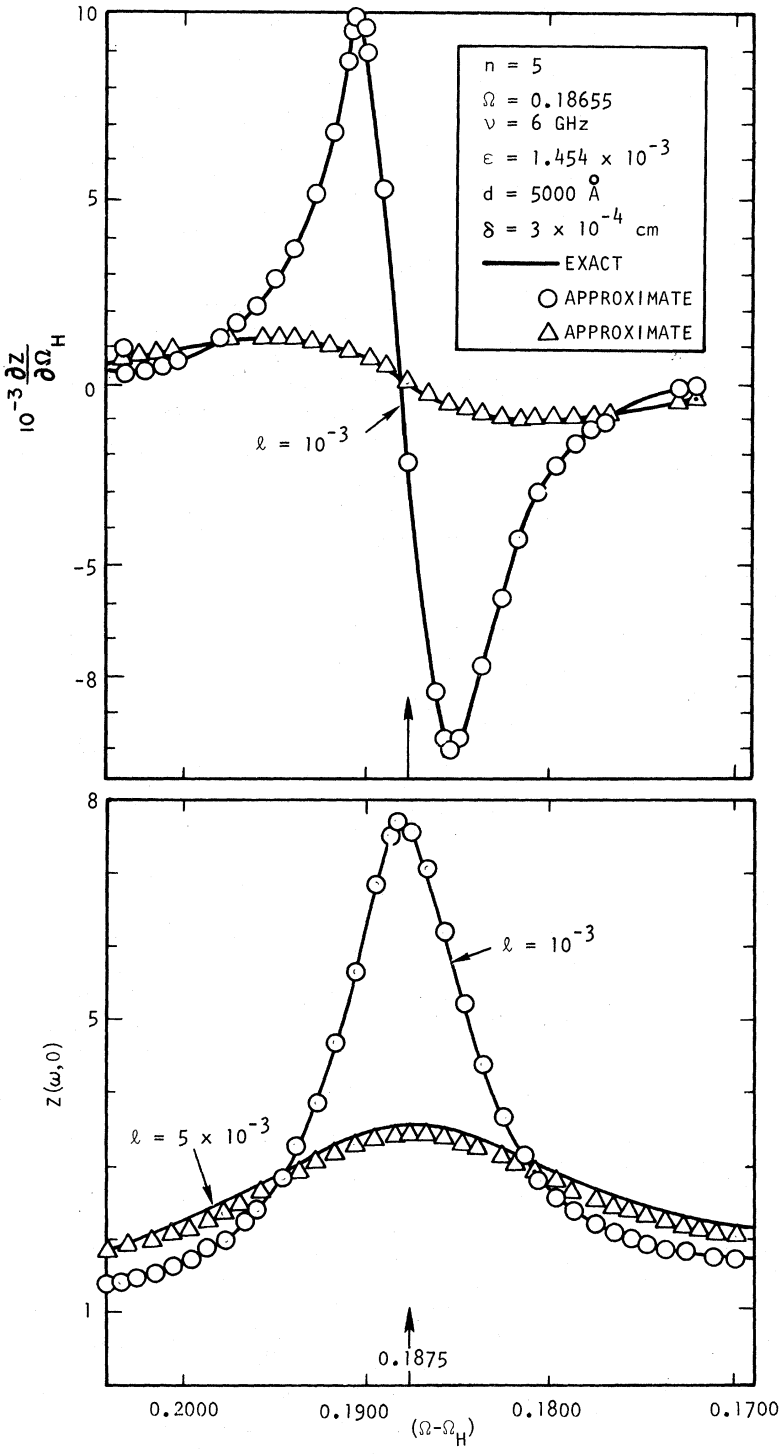

FIG. 5. Comparison of approximate and exact calculations of the derivative of the surface impedance (upper) and the surface impedance (lower) for $l=10^{-3}$ and $l=5\times10^{-3}$ for the $n=5$ spin-wave resonance in a 5×10^{3}-Å Permalloy film. The heavy curves are calculated from the exact formulas and the Δ and 0 are from the approximate formulas.

C. Spin-Wave Resonance Mode Intensities

With the aid of our approximation formula, Eq. (5.8), we can determine the peak heights and widths and also the derivative of power absorption peaks.

First we note that the SWRP contribution is in the form of a Breit-Wigner shape. The peak height at resonance a_n is

$$a_n = 4\frac{\delta}{d}\frac{|\alpha|\Omega}{\lambda_n\Gamma_n} = \frac{4(\delta/d)}{\lambda_n\Omega l/\epsilon^2+2} \quad . \tag{5.10}$$

We see that in the absence of magnetic losses the peak heights are constant. This result seems rather strange at first glance. One might expect

that the power absorption should fall off as $1/n^2$ because alternate half-wavelengths across the film cancel. The remaining uncompensated half-wavelength of the nth mode contributes only $1/n^2$ to the volume integral of Poynting's vector. The answer to this apparent contradiction is that the height of the peak in the power absorption is inversely proportional to the imaginary part of the eigenfrequency. According to Eq. (3.19) the imaginary part of the frequency $\Omega_{nI}(0)$ is proportional to $1/n^2$ when $d \ll \delta$ so that the decrease due to cancellation is exactly compensated by the decrease in $\Omega_{nI}(0)$ with increasing n. The decrease of the eddy-current losses as n increases exactly cancels the n^{-2} decrease in the peak heights due to the wave cancellation across the film. When $l \neq 0$ then the peak height is not constant. When the term $\lambda_n \Omega l/\epsilon^2 \gg 2$ then the peak height decreases as $1/n^2$. For the parameters previously mentioned $\lambda_n \Omega l/\epsilon^2 \approx 6.63 l n^2$. For $n=9$, $\lambda_n \Omega l/\epsilon^2 \approx 2$ for $l = 4\times 10^{-3}$. The modes with $n > 9$ will then be dominated by magnetic losses. The peak height is controlled by the prefactor (δ/d) which has a frequency dependence of $\omega^{-1/2}$ due to the skin depth. It might appear that the factor $\lambda_n \Omega l/\epsilon^2$ is also frequency dependent. This is not the case since $\epsilon^2 \propto 1/\delta^2 \propto \Omega$. In order to produce a frequency dependence in the ratio of the peak heights a_{n+1}/a_n using the Landau-Liftshitz form of damping, the damping parameter l would have to be frequency dependent.

The FMRB contribution to the peak height is small in thin films for the high-order modes when $l \lesssim 10^{-2}$. For the low-order modes the FMRB is important. This contribution increases with increasing frequency and decreases with n approximately as $1/n^2$.

In many cases the "peak-to-valley" amplitude difference in the derivative (with respect to the applied field) of the power absorption is used as a measure of the mode intensities. The difference in applied field value for the maximum and minimum in the derivative is used as a measure of the linewidth.

The principal contribution to the derivative comes from the SWRP function. The effect of the FMRB is to produce an asymmetry in the derivative. Near the main FMR peak the asymmetry is large. The derivative of the FMRB overwhelms the SWR contribution when $\Omega - \Omega_H \approx \epsilon$ so that a number of SWRP may be unresolved.

The derivative of the surface impedance is

$$\frac{\partial Z_{\text{total}}}{\partial \Omega_H} \approx \frac{-16(\delta/d)|\alpha|}{\lambda_n} \frac{\Omega^2(\omega_n^2 - \Omega^2)\Gamma_n}{[(\omega_n^2 - \Omega^2)^2 + \Gamma_n^2]^2} + \frac{d/\delta}{6}\left[\left(\frac{1}{\Omega - \Omega_H} - 1\right)^2 - \left(\frac{1}{\Omega + \Omega_H} - 1\right)\left(\frac{1}{\Omega + \Omega_H}\right)^2\right] . \tag{5.11}$$

This approximation is compared with that obtained by differentiation of Eq. (5.9) in Fig. 5. The agreement is excellent for the modes well removed from the FMR peak. We note that the maximum (minimum) in $\partial Z_{\text{total}}/\partial \Omega_H$ occurs at $\omega_n^2 - \Omega^2 = (\pm)\Gamma_n/\sqrt{3}$. The difference between the derivative maximum and minimum is

$$I_n \approx \frac{3\sqrt{3}}{8} \frac{\lambda_n}{|\alpha|}\left(\frac{d}{\delta}\right) a_n^2 \qquad (\Omega - \Omega_H \gg \epsilon) . \tag{5.12}$$

Thus the mode intensity I_n as calculated from the derivative decreases as $1/n^2$ when a_n decreases as $1/n^2$.

D. Effect of Thickness Variations

Experimental microwave power absorption usually shows that the linewidth of the higher-order modes is much larger than that predicted by theoretical models. One important factor that leads to a broadening of the higher-order modes is variations in film thickness. Thickness variations of the order of 30–50 Å are to be expected. For a 5000-Å film this gives $\Delta d/d \sim 1\%$. The simplest model which includes the effects of Δd is that in which the absorption spectrum is a superposition of spectra arising from many different sections of the film whose thickness is locally constant. Thus if $\langle Z^n \rangle$ is the observed superposition of spectra

$$\langle Z^n \rangle \approx \frac{1}{\Delta d}\int_{t_1}^{t_2} Z^n_{\text{SWRP}}(t)\, dt , \tag{5.13}$$

where t_2 and t_1 are the maximum and minimum film thickness, respectively, and $\Delta d = t_2 - t_1$. More sophisticated weighted averages can be imagined but the essential features of the effect can be seen in this simple linear model. Using Eq. (5.6) we obtain

$$\langle Z^n \rangle \approx \frac{-2(\delta/d)|\alpha|}{(\Delta d/d)\lambda_n^2}\left[\arctan\left(\frac{\omega_n^2(t_2) - \Omega^2}{\Gamma_n}\right) - \arctan\left(\frac{\omega_n^2(t_1) - \Omega^2}{\Gamma_n}\right)\right] . \tag{5.14}$$

The derivative gives

$$\frac{\partial}{\partial \Omega_H}\langle Z^n \rangle \approx -\left(\frac{d}{\Delta d}\right)\frac{1}{\lambda_n}\left[Z^n_{\text{SWRP}}(t_2) - Z^n_{\text{SWRP}}(t_1)\right] . \tag{5.15}$$

The two line shapes in Eq. (5.15) will be approximately resolved when the separation of the peaks is of the order of Γ_n, that is, when

$$\lambda_n\left(\frac{\Delta d}{d}\right) \geq \Gamma_n = 2\Omega\left(\Omega l + \frac{|\alpha|}{\lambda_n}\right) . \tag{5.16}$$

We note that for $\Delta d/d \sim 1\%$ this condition is easily satisfied. For example, with the parameters used previously and $l = 10^{-2}$ the inequality is satisfied for

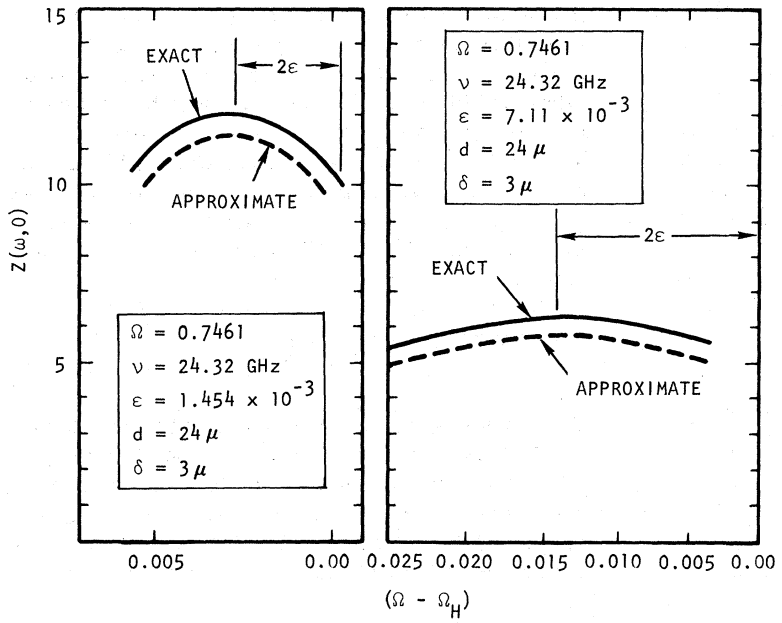

FIG. 6. Comparison of the exact and approximate formulas for the surface impedance at the ferromagnetic resonance peak for a film 24 μ in thickness. The constant difference is due to the neglect of the $Z^{(-)}$ contribution.

$n > 9$. For such a case according to Eq. (5.15) the derivative decreases as $1/n^4$ instead of $1/n^2$. This effect results from the fact that the resonance frequency now varies over a range due to thickness variations which increase as $n^2[\Delta\Omega_n \approx [2(D/4\pi) \times (\pi/d)\Delta d]n^2\}$. The total integrated intensity is approximately constant so that the peak height must decrease with an additional factor of n^{-2}. This factor also appears in the derivative of the intensity. We also note that the condition Eq. (5.15) is frequency dependent so that for low frequencies the $1/n^4$ behavior may be approached for smaller n than in the high-frequency case provided $\Omega l > |\alpha|/\lambda_n$ in both instances. Frequency dependences of this sort but even more pronounced have been reported recently by Weber and Tannenwald.[20]

The linewidth of $\langle Z^n \rangle$ is much broader than that of Z^n_{SWRP} for the typical thin film resonance experiment.

E. Characteristics of the FMR Peak

We commented earlier that the FMR peak position and height is controlled by the exchange interaction. When $d \gtrsim 4\delta$ the shape of the power absorption curve becomes independent of thickness. When d is large the quantities $\tan(k^{\pm}_{1,2} d/2) \to i$ provided that $k^{\pm}_{1,2} \neq 0$. For $\Omega \sim \Omega_H$ none of the propagation constants vanish and therefore we find that the power absorption tends to

$$Z_\infty(0) = \delta\left(\left|\frac{1-\frac{1}{2}i\delta^2 k_1^+ k_2^+}{\delta^2(k_1^+ + k_2^+)} + \frac{1-\frac{1}{2}i\delta^2 k_1^- k_2^-}{\delta^2(k_1^- + k_2^-)}\right|\right) . \tag{5.17}$$

The contribution due to the left-hand circularly polarized waves is nearly constant for $\Omega \sim \Omega_H$ while that due to the right-hand circularly polarized waves changes rapidly. Consequently the FMR peak position can be located by finding the maximum of the first term. Making use of Eq. (4.6) and the fact that the peak occurs when $|\eta|$ is of the order of ϵ we find that near the peak

$$Z_\infty^+ \approx \frac{1}{2}\frac{1-i}{[(\Omega' - \Omega_H - 2\epsilon) - i(2\epsilon + l\Omega')]^{1/2}} . \tag{5.18}$$

An approximately constant correction due to Z_∞^- must be added to the right-hand side of Eq. (5.18) in order to calculate the magnitude of Z_∞ accurately. The maximum occurs at $\Omega_H = \Omega' - 2\epsilon$. At this field the peak has the magnitude

$$\mathrm{Re}Z_\infty^+|_{\max} = \frac{1}{2(\epsilon + \frac{1}{2}l\Omega')^{1/2}} . \tag{5.19}$$

For small values of ϵ the Z_∞^- contribution is relatively small. In Fig. 6 the function Z_∞ according to Eq. (5.17) is compared with the approximation Z_∞^+ of Eq. (5.18). The constant difference of 0.65 is due to the lack of the Z_∞^- contribution.

Next we consider the dipolar dispersion of the FMR peak. Using Eq. (4.13)

$$Z(\omega, k_{\parallel}) = \frac{(2i/k)T_{11}}{|1+T_{11}|^2} \approx \frac{Z_\infty^+(0)}{|1+(k/2i)Z_\infty^+(0)|^2} . \tag{5.20}$$

For small values of $k_{\parallel}$ the peak position of $\mathrm{Re}Z(\omega, k_{\parallel})$ is given by

$$\Omega' - \Omega_H \approx 2\epsilon + \left(\frac{\epsilon}{2} + \frac{l\Omega'}{4}\right)^{1/2} K . \tag{5.21}$$

This result is valid only when $K\epsilon^{-1/2} < 1$. For larger values of K quadratic terms are important and the

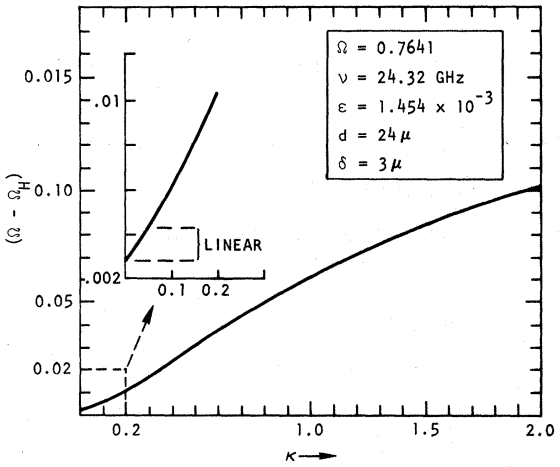

FIG. 7. The dipolar dispersion of the ferromagnetic resonance peak as a function of $K=\delta|k_{\parallel}|$. The small K region is described by $\Omega-\Omega_H=2\epsilon+(\epsilon/2+l\Omega'/4)^{1/2}$ in the linear region. This region is indicated in the enlarged small K region. The parameter $l=10^{-3}$.

relation is no longer linear. In Fig. 7 the dependence of the FMR peak on K is shown.

F. Antiresonance

Recent experiments have shown that the transmission of microwave energy through a ferromagnetic metal exhibits a maximum at $\omega=\gamma H_{app}$ or in our dimensionless units at $\Omega_H=\Omega-1$. This phenomenon is a result of the behavior of the magnetic susceptibility of the ferromagnetic medium. In the case we are considering of the applied magnetic field perpendicular to the sample surface the absorption minimum is associated with the behavior of $Z^+(\omega, k_{\parallel}=0)$ as is evident in Fig. 4.

To study this feature we note that according to Eq. (4.16) that if $l=0$ then $k_2^+\to 0$ as $\Omega_H\to\Omega-1$. The minimum in $Z^+(\omega, k_{\parallel}=0)$ is associated with $k_2^+\to 0$. For small l and $\eta-1$ small,

$$\delta^2\epsilon^2(k_1^+)^2\approx\eta-\alpha+\left(\frac{\eta-1}{\eta}\right)\alpha\,,$$
$$\delta^2\epsilon^2(k_2^+)^2\approx-\left(\frac{\eta-1}{\eta}\right)\alpha\,. \tag{5.22}$$

For the semi-infinite surface impedance of Eq. (5.17), $k_2^+\approx(-1+i)[(\eta-1)/n]^{1/2}$ when $l=0$ and $\eta-1>0$ while for $(\eta-1)<0$, $k_2^+\approx(1+i)[(1-\eta)/n]^{1/2}$ since the imaginary part of k_2^+ must be positive. The propagation vector k_2^+ as a function of η therefore has a cusp at $\eta-1=0$ and this behavior leads to a cusp in the surface impedance. When $l\neq 0$ the minimum in $Z^+(\omega, k_1=0)$ is parabolic as shown in Fig. 4.

It is tempting to suppose that $Z_\infty(0)$ can be used to study the antiresonance when $d\gg\delta$. The problem is that $Z_\infty(0)$ is obtained from Eq. (4.15) by replacing $\tan k_2^+ d/2$ by i, a procedure which is valid when $\mathrm{Im}(k_2^+ d/2)\gg 1$. However, at the antiresonance minimum $k_2^+\to 0$ and $\tan k_2^+ d/2$ may not be replaced by i near $\eta-1=0$. The presence of nonzero l does not remedy this problem. Thus Eq. (4.15) should be utilized in studying the antiresonance. For $l=0$ and $d\gg\delta$ we may evaluate $Z^+(\omega, k_{\parallel}=0)$ by using $k_2^+=0$ and $\tan k_1 d/2=i$. Then we find that the minimum value of $Z^+(\omega, k_{\parallel}=0)$ is

$$\mathrm{Re}Z_{\min}^+=\mathrm{Re}\left(\frac{\epsilon}{(1-\alpha)^{1/2}}\right)\approx\epsilon\,. \tag{5.23}$$

This should be compared to the maximum value of $\mathrm{Re}Z^+=1/2(\epsilon)^{1/2}$. Since $\epsilon\sim 10^{-3}$ we see that the minimum is many orders of magnitude smaller than the maximum. A detailed study of the antiresonance for both parallel and perpendicular resonance conditions will be presented elsewhere.

VI. SUMMARY OF RESULTS

In this section the important results derived in the main text are summarized. It is convenient first to recall the definitions of the various symbols.

$\hbar$ equals Planck's constant/2π; ω is the angular frequency in rad/sec; M_s is the saturation magnetization in Oe; Ω is the dimensionless frequency $\Omega=\hbar\omega/4\pi\gamma M_s$; γ equals the gyromagnetic ratio (erg/Oe); $\Omega_n(k_{\parallel})$ is the dimensionless frequency for the nth magnetoexchange branch of a metallic ferromagnet; $\tilde{\Omega}_n(k_{\parallel})$ is the dimensionless frequency for the nth magnetoexchange branch of an insulating ferromagnet; n is an integer; $\vec{k}_{\parallel}$ is a wave vector parallel to the sample surface; $K=\delta k_{\parallel}$ is a dimensionless in-plane propagation constant; δ is the electromagnetic skin depth; d is the sample thickness; Ω_H is the dimensionless internal field $\Omega_H=(H_{app}/4\pi M_s)-1$; H_{app} is the applied static magnetic field perpendicular to the sample surface; $(D/4\pi)$ is the exchange constant (cm^2); l is the phenomenological magnetic relaxation parameter; Ω_{ex} is the dimensionless exchange energy $(D/4\pi)k_{\parallel}^2$; c is the velocity of light; σ is the electrical conductivity; λ_n is the exchange energy $(D/4\pi)(\pi/d)^2n^2$; ϵ is the dimensionless parameter $(D/4\pi\delta^2)^{1/2}$; $p_{\perp}(\omega, k_{\parallel})$ is the power absorbed per unit surface area (cgs units); $Z(\omega, k_{\parallel})$ is the generalized surface impedance; $Z_{\mathrm{FMRB}}(\omega, k_{\parallel}=0)$ is the surface impedance associated with the ferromagnetic resonance and eddy currents; $Z^n_{\mathrm{SWRP}}(\omega, k_{\parallel}=0)$ is the surface impedance associated with the nth spin-wave resonance peak; Z^n_{total} is the total surface impedance $Z^n_{\mathrm{total}}=Z_{\mathrm{FMRB}}+Z_{\mathrm{SWRP}}$; and $Z_\infty^{\pm}(0)$ is the surface impedance of thick metallic films ($d\gg\delta$) for right- (+) or left- (−) hand circularly polarized h_{rf}.

A. Spin-Wave Modes

The spin-wave frequencies of a conducting ferromagnetic plate (magnetoexchange branches) as a function of $k_{\parallel}$ are

$$\Omega_n(k_{\parallel}) = \Omega_n(0) + (1+il)\left(\frac{2n^2\pi^2(\delta/d)^4}{[2i+n^2\pi^2(\delta/d)^2]^2}\right)k_{\parallel}d\,, \tag{6.1}$$

where

$$\Omega_n(0) = \{(\Omega_H+\lambda_n) + (2i)[2i+n^2\pi^2(\delta/d)^2]^{-1}\}(1+il) \tag{6.2}$$

and

$$\lambda_n = n^2\pi^2(D/4\pi)(1/d)^2\,.$$

For the insulating ferromagnetic plate

$$\tilde{\Omega}_n(k_{\parallel}) = (\Omega_H+\lambda_n)(1+il) + \begin{cases} \dfrac{2}{n^2\pi^2}\,k_{\parallel}d(1+il) & \text{for } n=1,3,5\ldots \\ \Omega_{ex} + \dfrac{3}{2}\left(\dfrac{k_{\parallel}d}{n\pi}\right)^2(1+il) & \text{for } n=2,4,6\ldots \end{cases} \tag{6.3}$$

Equations (6.1) and (6.3) are valid when the spacing between $k_{\parallel}=0$ levels is large compared to the dispersion.

B. Power Absorption in Thin Films

The generalized surface impedance is related to the average power absorbed by

$$P_{\perp}(\omega, k_{\parallel}) = \left(\frac{c}{4\pi\delta\sigma}\right)\mathrm{Re}\,Z(\omega, k_{\parallel})\,. \tag{6.4}$$

The surface impedance near the nth microwave absorption peak for $k_{\parallel}=0$ is

$$Z^n_{\text{total}} \approx \left(4\,\frac{\delta}{d}\,\frac{|\alpha|}{\lambda_n}\,\Omega\right)\frac{\Gamma_n}{(\omega_n^2-\Omega^2)+\Gamma_n^2} + \frac{(d/\delta)^2}{12}\left[\left(\frac{1}{\Omega-\Omega_H}-1\right)^2+\left(\frac{1}{\Omega+\Omega_H}+1\right)^2\right], \tag{6.5}$$

where $\alpha = 2i\epsilon^2$, $\epsilon^2 = D/4\pi\delta^2$, $\omega_n = \Omega_H+\lambda_n$, and $\Gamma_n = 2\Omega(\Omega l + |\alpha|/\lambda_n)$. Equation (6.5) applies to films with $d \ll \delta$ in the range

$$\lambda_{n+1} - \lambda_n \geq 2(\Omega_H - \Omega_n) \geq \lambda_n - \lambda_{n-1}$$

for each branch $n=1, 2, \ldots$ when $\Omega - \Omega_H \gg \epsilon$. The peak height a_n of the nth ($k_{\parallel}=0$) standing spin-wave absorption peak of a thin film is given by

$$a_n = 4(\delta/d)(2+\lambda_n\Omega l/\epsilon^2)^{-1}\,. \tag{6.6}$$

The derivative of the surface impedance of the nth spin-wave mode is approximately

$$\frac{\partial Z^n_{\text{total}}}{\partial\Omega_H} \approx \frac{-16(\delta/d)|\alpha|\Omega^2(\omega_n^2-\Omega^2)\Gamma_n}{\lambda_n[(\omega_n^2-\Omega^2)^2+\Gamma_n^2]^2} + \frac{(d/\delta)^2}{6}\left[\left(\frac{1}{\Omega-\Omega_H}-1\right)\left(\frac{1}{\Omega-\Omega_H}\right)^2 - \left(\frac{1}{\Omega+\Omega_H}-1\right)\left(\frac{1}{\Omega+\Omega_H}\right)^2\right]\,. \tag{6.7}$$

The difference between the maximum and minimum of the derivative of the surface impedance is

$$I_n \approx \frac{3\sqrt{3}}{8}\,\frac{\lambda_n}{|\alpha|}\left(\frac{d}{\delta}\right)a_n^2\,, \tag{6.8}$$

where a_n is given by Eq. (6.6).

C. Power Absorption in Thick Films

For thick ($d \gg \delta$) metallic films the $k_{\parallel}=0$ surface inpedance near the FMR peak is described by

$$Z^+_{\infty}(0) \approx \frac{\frac{1}{2}(1-i)}{[(\Omega'-\Omega_H-2\epsilon)-i(2\epsilon+l\Omega')]^{1/2}}\,, \tag{6.9}$$

where $\Omega' = \Omega/(1+l^2)$. The maximum in the FMR peak occurs at $\Omega_H = \Omega' + 2\epsilon$ and has the value $[2(\epsilon+\frac{1}{2}l\Omega')]^{1/2}$.

The dipolar dispersion of the FMR peak is initially linear with K for small K. This dispersion is described by

$$\Omega' - \Omega_H = 2\epsilon + \left(\frac{\epsilon}{2}+\frac{l\Omega'}{4}\right)^{1/2}K\,, \tag{6.10}$$

when $K\epsilon^{1/2} < 1$. A power absorption minimum occurs at $\Omega_H \approx \Omega - 1$. The surface impedance at this antiresonance is approximately equal to ϵ when $l \ll \epsilon$.

[1] J. H. E. Griffiths, Nature 158, 670 (1946).

[2] W. A. Yager and R. M. Bozorth, Phys. Rev. 72, 80 (1947); see also J. A. Young, Jr. and E. A. Uehling, *ibid.* 94, 544 (1954); N. Bloembergen, *ibid.* 78, 572 (1950).

[3] C. Kittel, Phys. Rev. 71, 270 (1947); 73, 155 (1948).

[4] G. T. Rado and J. R. Weertman, Phys. Rev. 94, 1386 (1954); J. R. Weertman, J. Appl. Phys. 29, 328 (1958).

[5] W. S. Ament and G. T. Rado, Phys. Rev. 97, 1558 (1955).

[6] M. H. Seavey, Jr. and P. E. Tannenwald, Phys. Rev. Letters 1, 168 (1958); J. Phys. Radium 20, 323 (1959).

[7] See, for example, C. F. Kooi, P. E. Wigen, M. R. Shanabarger, and J. V. Kerregan, J. Appl. Phys. 35, 791 (1961); M. Nisenoff and R. W. Terhune, *ibid.* 36,

732 (1965); R. Weber and P. E. Tannenwald, Phys. Rev. 140, A498 (1965).

[8]C. Kittel, Phys. Rev. 110, 1295 (1958); P. Pincus, *ibid.* 118, 658 (1960); J. W. Hartwell, Proc. IEEE 56, 23 (1968).

[9]The angular dependence of ferromagnetic resonance has also been examined. C. Vittoria, R. C. Barker, and A. Yelon, J. Appl. Phys. 40, 1561 (1969). See also Ref. 10.

[10]R. F. Soohoo, J. Appl. Phys. Suppl. 32, 148S (1961).

[11]G. I. Lykken, Phys. Rev. Letters 19, 1431 (1967).

[12]M. Sparks, B. R. Tittmann, J. E. Mee, and C. Newkirk, J. Appl. Phys. 40, 1518 (1969).

[13]R. E. De Wames and T. Wolfram, J. Appl. Phys. 41, 987 (1970).

[14]T. G. Phillips, L. W. Rupp, Jr., A. Yelon, R. C. Barker, and C. Vittoria, J. Phys. (Paris) 32, C1-1162 (1971).

[15]O. Horan, G. C. Alexandrakis, and C. N. Manicopoulos, Phys. Rev. Letters 25, 246 (1970); B. Heinrich and V. F. Meshcheryakov, Zh. Eksperim. i Teor. Fiz. Pis'ma v Redaktsiyu 9, 618 (1969) [Sov. Phys. JETP Letters 9, 378 (1969)].

[16]See, for example, A. I. Akhiezer, V. G. Bar'yakhar, and S. V. Pepetimnski, *Spin Waves* (North-Holland, Amsterdam, 1969).

[17]The matrix treatment of the boundary conditions was suggested by R. L. Walker (private communication).

[18]R. E. DeWames and T. Wolfram, Phys. Rev. Letters 26, 1445 (1971); T. Wolfram and R. E. De Wames, Solid State Commun. 9, 171 (1971).

[19]See, for example, P. M. Morse and H. Feshback, *Methods of Theoretical Physics* (McGraw-Hill, New York, 1953), Vol. 1, p. 215.

[20]R. Weber, P. E. Tannenwald, and C. H. Bajorek, Appl. Phys. Letters 16, 35 (1970).

PHYSICAL REVIEW B VOLUME 4, NUMBER 9 1 NOVEMBER 1971

Two-Exciton Transitions in MnF_2 and $RbMnF_3$

S. E. Stokowski, D. D. Sell, and H. J. Guggenheim
Bell Telephone Laboratories, Murray Hill, New Jersey 07974

(Received 9 June 1971)

Absorption lines corresponding to the simultaneous creation of two excitons have been investigated in MnF_2 and $RbMnF_3$. The particular zero-phonon transitions observed are those from the ground states of a Mn ion pair to the $^4T_1(G)+{}^4T_1(G)$, $^4T_1(G)+{}^4A_1$, ^4E, and $^4T_1(G)+{}^4T_2(D)$ excited states in MnF_2 and to the $^4T_1(G)+{}^4T_1(G)$, $^4T_1(G)+{}^4A_1$, ^4E, and $^4A_1$, $^4E+{}^4A_1$, ^4E states in $RbMnF_3$. An attempt is made to identify the particular excitons created in these transitions through their polarizations and uniaxial stress behavior. Selection rules are derived using the space-group representations along with the additional assumption that the transition mechanism is an off-diagonal exchange interaction between pairs of Mn ions on opposite magnetic sublattices. The interaction between excitons is discussed; it is found experimentally that for those excitons which couple strongly to the lattice, the phonon coupling provides the major part of the interaction. The exciton-exciton interaction energy is positive or negative and varies from 10 to 400 cm^{-1} in magnitude. A measurement of the L-point magnon energy in $RbMnF_3$ has been made from an analysis of the $^6A_1 \rightarrow {}^4T_1(G)$ magnon sidebands; it is found to be 73 ± 0.5 cm^{-1}.

I. INTRODUCTION

The creation of more than one quasiparticle upon the absorption of a photon is a general feature in the spectra of many solids and occurs whenever there is an interaction between the quasiparticles. The quasiparticles about which we are speaking could be, for example, phonons, excitons, or magnons. By definition, photon absorption involving the creation of several quasiparticles is weak, since presumably the particle states have been constructed so that the two-particle interactions are small. However, if the one-particle transition is forbidden in some way, the pair or multiple transitions can be a relatively important feature in the absorption spectrum. Two-particle or pair transitions have been observed in the spectra of antiferromagnetic insulators, α-O_2,[1] and possibly silicon.[2] Pair transitions have also been seen for pairs of impurity ions in solids.[3-5]

The pair transitions in antiferromagnetic insulators have been studied in considerable detail. These transitions include combinations of two important quasiparticles present in magnetic systems: magnons and excitons. The absorption spectra of these substances exhibit exciton-magnon,[6,7] two-magnon,[8] and two-exciton transitions.[9] These processes have been of interest because of their intimate relationship with the exchange interaction between ions. Further, they have been useful in studying the properties of excitons and magnons. In this paper we shall concern ourselves with the two-exciton transitions in MnF_2 and $RbMnF_3$.

This work was motivated by our earlier work[10] on two-exciton lines in MnF_2, in which the lowest two-exciton states were observed and identified. In order to understand the source of the interaction between excitons and the strengths of the two-ex-